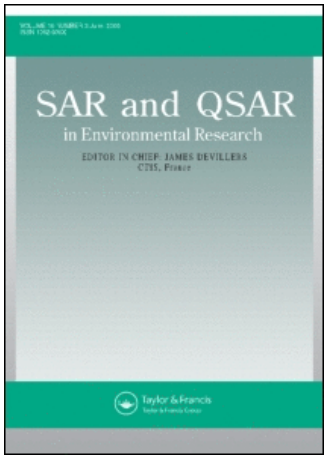

SAR and QSAR in Environmental Research
Publication details, including instructions for authors and subscription information:
http://www.informaworld.com/smpp/title~content=t716100694

QSAR and pharmacophore analysis on amides against drug-resistant **S. aureus**

I. Yildiz [a]; T. Ertan [a]; K. Bolelli [a]; O. Temiz-Arpaci [a]; I. Yalcin [a]; E. Aki [a]
[a] Faculty of Pharmacy, Department of Pharmaceutical Chemistry, Ankara University, Tandogan, Ankara, Turkey

Online Publication Date: 01 January 2008
To cite this Article: Yildiz, I., Ertan, T., Bolelli, K., Temiz-Arpaci, O., Yalcin, I. and Aki, E. (2008) 'QSAR and pharmacophore analysis on amides against drug-resistant **S. aureus** ', SAR and QSAR in Environmental Research, 19:1, 101 - 113
To link to this article: DOI: 10.1080/10629360701844159
URL: http://dx.doi.org/10.1080/10629360701844159

SAR and QSAR in Environmental Research
Vol. 19, Nos. 1–2, January–March 2008, 101–113

QSAR and pharmacophore analysis on amides against drug-resistant *S. aureus*[1]

I. Yildiz*, T. Ertan, K. Bolelli, O. Temiz-Arpaci, I. Yalcin and E. Aki

Faculty of Pharmacy, Department of Pharmaceutical Chemistry, Ankara University, Tandogan, Ankara, Turkey

(*Received 1 September 2007; In final form 11 November 2007*)

Considering the worth of developing new antibacterial agents against drug-resistant *Stapylococcus aureus*, the present study explores the structure-activity relationships analysis of *N*-(2-hydroxy-4(or 5)-nitro/aminophenyl)benzamide and phenylacetamide derivatives using classical QSAR and 3D-common-feature pharmacophore hypothese approaches. QSAR analysis revealed that the compounds possessing a methylene group between the phenyl and the carboxyamido moiety played a role for decreasing the activity. On the other side, substituent effects on position R_1 was found important for the activity and holding a substituent possessing a minimum width property on this position like as alkyl groups enhanced the activity. Moreover, substituting position R_3 with a group enhancing the electron-donor capability of the phenolic ring system increased the potency. 3D-common-feature pharmacophore approach considered that the conformational properties of the compounds were important for the activity against drug-resistant *S. aureus* and compounds possessing a benzamide moiety rather than phenylacetamide structure increased the activity. Furthermore, holding NO_2 and OH groups on the phenyl ring attached to the benzamide moiety was important for improving the potency against drug-resistant *S. aureus*.

Keywords: benzamide; phenylacetamide; drug-resistant *Staphylococcus aureus*; QSAR; 3D-common-feature pharmacophore hypotheses; hiphop

1. Introduction

The dramatically rising prevalence of multi-drug resistant microbial infections in the past few decades has become a serious health care problem. In particular, the emergence of multi-drug resistant strains of Gram-positive bacterial pathogens such as methicillin-resistant *Staphylococcus aureus* and *S. epidermis* and vancomycin-resistant *Enterococcus* is a problem of ever-increasing significance [1–5]. In order to prevent this serious medical problem, the elaboration of the new types of the previously known drugs is a very actual task.

Benzamide derivatives exhibit various types of biological properties such as anthelmintic, antihistaminic, antifungal, and antibacterial [6–14]. 6-*N*-(2-hydroxy-3,5-dichlorophenyl)-2-hydroxy-3,5,6-trichlorobenzamide (Oxyclozanide), which has a

*Corresponding author. Email: iyildiz@pharmacy.ankara.edu.tr
[1]Presented at CMTPI 2007: Computational Methods in Toxicology and Pharmacology Integrating Internet Resources (Moscow, Russia, September 1–5, 2007).

ISSN 1062–936X print/ISSN 1029–046X online

DOI: 10.1080/10629360701844159
http://www.informaworld.com

benzamide structure, was discovered in 1969 as an anthelmintic agent effective against *Fasciola hepatica* for the treatment of liver fluke infection [6]. 3,4-Dihydroxy-6-(*N*-ethylamino)benzamide is a natural product that has been found in green pepper (*Piper nigrum* L.) as an antibacterial by Pradhan et al. in 1999 [11].

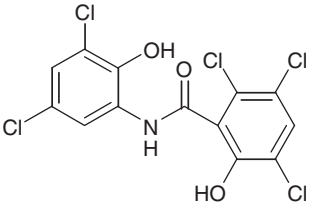

Oxyclozanide

Additionally, a benzamide derivative, BAS-118, has been found to be a novel anti-*Helicobacter pylori* agent with a potent and selective antibacterial activity, which includes clarithromycin (CAM)- and metronidazole (MNDZ)-resistant isolates [15].

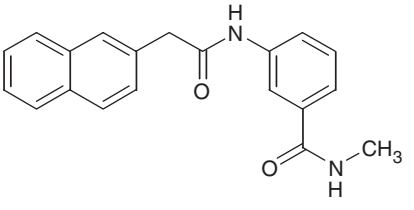

BAS-118

In the drug design area, quantitative structure-activity relationship (QSAR) modelling is an area of research pioneered by Hansch and Leo [16] and Hansch and Fujita [17]. The QSAR method assumes that differences in the structural or physical properties measured experimentally account for differences in the observed biological or chemical properties [16–19]. A QSAR study usually leads to a predictive formula and attempts to model the activity of a series of compounds using measured or computed properties of the compounds. More recently, QSAR has been extended by including 3D information. In drug discovery, it is common to have measured activity data for a set of compounds acting upon a particular protein, but not to have knowledge of the three dimensional (3D) structure of the active site. In the absence of such 3D information, one may attempt to build a hypothetical model of the active site that can provide insight on the nature of the latter. Three-dimensional approaches such as HypoGen and/or HipHop are useful in building 3D pharmacophore models from the activity data and conformational structure [20]. It can be used as an alternative for QSAR methods because of easy visualization and high prediction capability. However, ranging activity values of a collection of conformational models of compounds should be at least four orders of magnitude for this algorithm, HypoGen. The other algorithm in 3D pharmacophore generation within Catalyst is called HipHop and is based on alignment of common features present in highly potent compounds. The scalar affinity values of the molecules are not regarded in this model generation mode. HipHop pharmacophore models are derived by comparing a set of conformational

models and a number of 3D configurations of chemical features shared among the training set molecules.

Because of the need of new antibacterial drugs active against the multi-drug resistant bacteria, recently, we have synthesized *N*-(2-hydroxy-4(or 5)-nitro/aminophenyl)benzamide and phenylacetamide derivatives (Table 1) as a new class of antimicrobial agents and reported their *in vitro* antibacterial activity against *Staphylococcus aureus* strains showing multi-drug resistance to oxacilin, gentamycin, aztreonam, and trimethoprim sulfamethoxazole [21]. Their antibacterial activities were observed as minimum inhibitory concentration (MIC) expressed in $\mu g\,ml^{-1}$ and the MIC values were determined by using the twofold serial dilution technique in Mueller-Hinton broth.

The aim of this study was to derive QSARs from multivariable regression analysis (MRA) in order to investigate the quantitative effect of structural properties of the molecules on their antibacterial activity against drug-resistant *S. aureus* strains and to

Table 1. Chemical structure and antibacterial activity of benzamide and phenylacetamide derivatives against drug-resistant *S. aureus* [21].

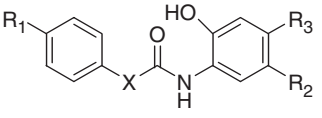

Comp. Nos	R_1	R_2	R_3	X	*MIC** $\mu g\,ml^{-1}$
1	$C(CH_3)_3$	H	NO_2	–	1.95
2	H	H	NO_2	–	125
3	F	H	NO_2	–	15.6
4	C_2H_5	H	NO_2	–	125
5	H	NO_2	H	–	15.6
6	C_2H_5	NO_2	H	–	7.8
7	F	NO_2	H	–	15.6
8	Br	H	NO_2	CH_2	125
9	Cl	H	NO_2	CH_2	125
10	CH_3	H	NO_2	CH_2	500
11	F	H	NO_2	CH_2	62.5
12	CH_3	NO_2	H	CH_2	125
13	F	NO_2	H	CH_2	31.25
14	$C(CH_3)_3$	H	NH_2	–	7.8
15	H	H	NH_2	–	15.6
16	F	H	NH_2	–	15.6
17	Br	H	NH_2	–	7.8
18	C_2H_5	H	NH_2	–	7.8
19	H	NH_2	H	–	31.25
20	C_2H_5	NH_2	H	–	15.6
21	F	NH_2	H	–	15.6
22	Br	H	NH_2	CH_2	31.25
23	Cl	H	NH_2	CH_2	31.25
24	CH_3	H	NH_2	CH_2	62.5
25	F	H	NH_2	CH_2	62.5
26	CH_3	NH_2	H	CH_2	62.5
27	F	NH_2	H	CH_2	31.25

Note: *Minimum Inhibitory Concentration.

generate common-features pharmacophore hypotheses by using Catalyst 4.9/HipHop [22] for finding the chemical features among a set of some antibacterial active benzamide and phenylacetamide derivatives.

2. QSAR analysis

Chemical structures and antibacterial activity against drug-resistant *S. aureus* strains of the previously synthesized compounds [21] shown as MIC values, are given in Table 1. The potency was defined as $\log 1/C$ where C was the MIC value expressed in molar concentration units. A training set including compounds **1**, **2**, **5**–**9**, **12**, **15**, **16**, **18**–**26** and a test set consisting in compounds **3**, **4**, **10**, **11**, **13**, **14**, **17**, **27** were considered. The variables used as independent descriptors in the QSAR analysis were hydrophobic, electronic, steric, and structural parameters. The structural variable I_x expresses a value of 1 for the presence of CH_2 group as a bridge element and 0 for the absence of it between phenyl and carboxyamido moiety. The screened physicochemical parameters in this QSAR study are $\log P$, π for the hydrophobic effects, σ, F (field effect), R (resonance effect), as the electronic influences and Verloop's STERIMOL descriptors (L, B_1, B_4) for the steric interactions of the substituents R_1, R_2 and R_3. Additionally, H-bond donor, H-bond acceptor and the other Free-Wilson type structural indicator variables were also used for positions R_2 and R_3 such as IR_2a (IR_3a), IR_2b (IR_3b) represented by a value of 1 for the presence of NO_2, NH_2 and 0 for the absence, respectively. Values of the physicochemical parameters used in this QSAR study were taken from the Table of Hansch and Leo [23] except $\log P$, which was calculated by using the Acclerys's Cerius2 [24] program. The values of the parameters used in the correlation equation related to the activity among the candidate set of variables in the training set are shown in Table 2. MRA was run on a PC using the BILIN [25] and MINITAB 13.1 [26] program packages.

MRA that involves finding the best fit of dependent variable (antibacterial activity) to a combination of independent variables (descriptors) was performed from least squares method.

The tabulated $F_{(3,15,0.95)}$ was 3.29 whereas the overall F test values for the obtained equation was 47.486 which is statistically significant at the 5% level of probability [27]. The statistically significant correlation equation (Equation (1)) obtained from MRA to describe the QSAR analysis is given below.

$$\log \frac{1}{C} = 0.95(\pm 0.24)\, B1_{R1} - 0.94(\pm 0.18)\, Ix - 0.37(\pm 0.16)\, \sigma R_3 + 2.92(\pm 0.35)$$
$$n = 19,\ r^2 = 0.905,\ s = 0.166,\ F = 47.486,\ t = 17.87,\ Q^2 = 0.820,\ s\text{-PRESS} = 0.228 \quad (1)$$

In Equation (1), the figures in parentheses are the standard errors of the regression coefficients, n is the number of compounds, r^2 is the square of multiple correlation coefficient, F is the significance test and s is the standard error of estimate.

In order to judge the validity of the predictive power of the QSAR analysis, the cross-validation method was also applied to the original data set by removing a compound from the data in such a way that each observation (compound) is deleted only once. For each reduced data set a model was developed and the response values of the deleted observations were predicted from this model and finally the resulting PRESS (predictive residual sum of squares) and Q^2 (the square of predictive power of coefficient) were calculated for the equation [28, 29]. The search for the simple correlation coefficients

Table 2. Training set of compounds, biological activity and parameters used in Equation (1).

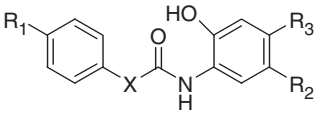

Comp. Nos	R_1	R_2	R_3	X	*MIC* $\mu g\,ml^{-1}$	*Ix*	σR_3	$B1_{R1}$
1	$C(CH_3)_3$	H	NO_2	–	1.95	0	0.78	2.59
2	H	H	NO_2	–	125	0	0.78	1
5	H	NO_2	H	–	15.6	0	0	1
6	C_2H_5	NO_2	H	–	7.8	0	0	1.52
7	F	NO_2	H	–	15.6	0	0	1.35
8	Br	H	NO_2	CH_2	125	1	0.78	1.95
9	Cl	H	NO_2	CH_2	125	1	0.78	1.80
12	CH_3	NO_2	H	CH_2	125	1	0	1.52
15	H	H	NH_2	–	15.6	0	−0.66	1
16	F	H	NH_2	–	15.6	0	−0.66	1.35
18	C_2H_5	H	NH_2	–	7.8	0	−0.66	1.52
19	H	NH_2	H	–	31.25	0	0	1
20	C_2H_5	NH_2	H	–	15.6	0	0	1.52
21	F	NH_2	H	–	15.6	0	0	1.35
22	Br	H	NH_2	CH_2	31.25	1	−0.66	1.95
23	Cl	H	NH_2	CH_2	31.25	1	−0.66	1.80
24	CH_3	H	NH_2	CH_2	62.5	1	−0.66	1.52
25	F	H	NH_2	CH_2	62.5	1	−0.66	1.35
26	CH_3	NH_2	H	CH_2	62.5	1	0	1.52

Table 3. Correlation matrix of the variables used in Equation (1).

	Ix	σR_3	$B1_{R1}$
Ix	1.000	0.090	0.374
σR_3		1.000	0.271
$B1_{R1}$			1.000

which are given in Table 3 also reveals that there is no intercorrelation between the independent variables in any case entered in the correlation equations. The calculated $\log 1/C$ values with residuals of the training set determined from Equation (1) are given in Table 4.

3. Common-feature pharmacophore hypotheses generation

All computational experiments were conducted on a Silicon Graphics O2, running under the IRIX 6.5 operating system. Hypotheses generation was applied against previously described data sets by using Catalyst/HipHop (version 4.9) from Accelrys 22. Molecules were edited using the Catalyst 2D/3D visualizer. Catalyst automatically generated conformational models for each compound using the Poling Algorithm 30–32. The ''best conformer generation'' procedure was applied to provide the best conformational

Table 4. Observed and calculated $\log 1/C$ values with residuals obtained from Equation (1).

Comp. Nos	*Observed log 1/C*	*Predicted log 1/C*	*Residuals*
1	5.207	5.091	0.116
2	3.315	3.578	−0.263
5	4.219	3.869	0.350
6	4.563	4.363	0.200
7	4.248	4.202	0.046
8	3.448	3.544	−0.096
9	3.389	3.402	−0.013
12	3.360	3.426	−0.066
15	4.165	4.114	0.051
16	4.198	4.447	−0.249
18	4.516	4.609	−0.093
19	3.863	3.869	−0.006
20	4.215	4.363	−0.148
21	4.198	4.202	−0.004
22	4.012	4.081	−0.069
23	3.946	3.938	0.008
24	3.612	3.672	−0.060
25	3.619	3.510	0.109
26	3.612	3.426	0.186

coverage for a maximum number of conformers generated defaulted to 250 in a 0–25 kcal mol^{-1} range from the global minimum. The generated conformations were used to align common molecular features and generate pharmacophore hypothesis. HipHop was used to the conformations generated to align chemically important functional groups common to the molecules in the study set. A pharmacophoric hypothesis then was generated from these aligned structures.

HipHop provides feature-based alignment of a collection of compounds without considering the activity. It matches the chemical features of a molecule, against drug candidate molecules. HipHop takes a collection of conformational models of molecules and a selection of chemical features, and produces a series of molecular alignments in a variety of standard file formats. HipHop begins by identifying configurations of features common to a set of molecules. A configuration consists of a set of relative locations in 3D space and associated feature types. A molecule matches the configurations if it possesses conformations and structural features that can be superimposed within a certain tolerance from the corresponding ideal locations. HipHop also maps partial features of molecules in the alignment set. This provision gives the option to use partial mapping during the alignment. Partial mapping allows to identify larger, more diverse, more significant hypotheses and alignment models without the risk of missing compounds that do not have to map to all of the pharmacophore features.

In this research, HipHop common feature hypotheses were generated to explain the specification of the antibacterial agents against drug-resistance *S. aureus*. This tool builds hypotheses (overlaying common features) for which the fit of individual molecules to a hypothesis can be correlated with activity of the molecule. A set of 12 active compounds from Table 1 was selected as the target training set (Table 5). Among the selected

Table 5. Selected active compounds and characteristics for the common feature hypothesis run.

Compounds	*Confs*[a]	*Features/ Confs*[a]	*Principal*[b]	*MaxOmitFeat*[c]
1	38	9.50	2	0
3	9	8.56	1	2
5	12	7.75	1	2
6	23	8.83	1	2
7	19	8.42	1	2
14	9	9.33	1	2
15	7	8.43	1	2
16	9	9.22	1	2
17	7	8.29	1	2
18	26	8.88	1	2
20	18	9.06	1	2
21	13	9.00	1	2

Notes: [a]Confs = number of conformers; Features/Confs = total number of features divided by the number of conformers (summed over the entire family of conformers).
[b]Principal = 1 means that this molecule must map onto the hypotheses generated by the search procedure. Partial mapping is allowed. Principal = 2 means that this is a reference compound. The chemical feature space of the conformers of such a compound is used to define the initial set of potential hypotheses.
[c]The MaxOmitFeat column specifies how many hypothesis features must map to the chemical features in each compound. A 0 in this column forces mapping of all features, a 2 allows hypotheses to which no compound feature map.

12 molecules, the most active molecule, compound **1**, was chosen as the reference, which should allowed to map all features on the generated hypotheses for the antibacterial activity against drug-resistant *S. aureus*.

The geometry of each compound was built with a visualizer and optimised by using the generalized CHARMm-like force field implemented in the program. A preparative test was performed with hydrogen-bond acceptor (HBA), hydrogen-bond acceptor lipid (HBAI), hydrogen-bond donor (HBD), hydrophobic (Hp), hydrophobic aromatic (HpAr), hydrophobic aliphatic (HpAl), negative ionisable (NI), positive ionisable (PI) and Ring Aromatic (R) 33. NI and PI were used rather than negative charge and positive charge in order to broaden the search for deprotonated and protonated atoms or groups at physiological pH. By using conformational poling [32], a representative family of conformers was generated, within a 25 kcal mol^{-1} range of the computed minimum, for each molecule. Potential hypothesis models were produced with the minimum permitted interfeature spacing of 2.00 Å generating alignments of common features [34] that included the projected points of HpAr, HBAI, and HBD [33]. The characteristics of the generated potential 10 hypotheses are listed in Table 6 and all the hypotheses contain three features except first hypothesis, which has four features concerning of HpAr, HBD, and two HBAl with the ranking score of 92.8337. Consequently, because of showing the highest ranking score and having more features, hypothesis 1 has been chosen for the further evaluation among the other generated potential hypotheses.

Table 6. Results of the common feature hypothesis run.

Hypotheses	*Feature*[a]	*Rank score*	*Direct hit*[b]	*Partial hit*[b]
1	HpAr HBD HBAl HBAl	92.8337	101011111101	010100000010
2	HpAr HBAl HBAl	85.3298	111111111111	000000000000
3	HpAr HBAl HBAl	85.3298	111111111111	000000000000
4	HpAr HBAl HBAl	81.0086	111111111111	000000000000
5	HpAr HBAl HBAl	80.2992	111111111111	000000000000
6	HpAr HBAl HBAl	78.1941	111111111111	000000000000
7	HpAr HBD HBAl	77.0525	111111111111	000000000000
8	HpAr HBAl HBAl	76.8021	111111111111	000000000000
9	HpAr HBD HBAl	76.8021	111111111111	000000000000
10	HpAr HBAl HBAl	76.4293	111111111111	000000000000

Notes: [a]HpAr = Hydrophob aromatic; HBAl = Hydrogen-bond acceptor lipid; HBD = Hydrogen-bond donor.
[b]Direct hit, all the features of the hypothesis are mapped. Direct Hit = 1 means yes; Partial Hit, partial mapping of the hypothesis. Partial Hit = 0 means no. Each number refers to a molecule in Table 5 (same order).

4. Discussion

The QSAR analysis in this study was performed using the extra-thermodynamic method, correlating the antibacterial activity against drug-resistant *S. aureus* with various physicochemical parameters in order to reveal predictions for the lead optimisation in the training set of compounds of *N*-(2-hydroxy-4(or 5)-nitro/aminophenyl)benzamides and phenylacetamides.

Results of QSAR analysis obtained by the MRA of the training set of compounds given in Table 2 demonstrate that the best equation (Equation (1)) is statistically significant.

As can be deduced from Figure 1, the goodness-of-fit of Equation (1) is very significant, possessing a high r^2 (90.5%) and a small s (0.166) with an overall F test value of 47.486 at the significant level of $p < 0.05$. From a statistical point of view, this equation has a sufficient number of degrees of freedom (DF = 15; see Table 7) that can be judged significant for overall F and t statistics at the 5% level of probability. As shown in Table 7, all the included variables in the best equation possess t values >2.131 (the tabulated t value for DF = 15; 95% significance level), confirming that the confidence intervals of all individual regression coefficients are justified at the 95% significance level [35, 36].

In order to avoid the risk of chance correlation, some circumstances which were pointed out by Kubinyi [37], have been taken into consideration in the study. Cross-validation was applied to the original data set and the resulting PRESS was calculated. The calculated overall PRESS values for Equation (1) is 0.228 that is found smaller than the SSY (sum of the squares of the response values of the total observations) values of the observed Equation (1), which is 4.3195 (see Table 7). This proves that the developed models predicted better than chance and can be considered statistically significant [29]. The ratio PRESS/SSY for Equation (1), which is the approximate confidence interval for a prediction, are smaller than 0.4 and it also provides proof that the observed models are valid [29].

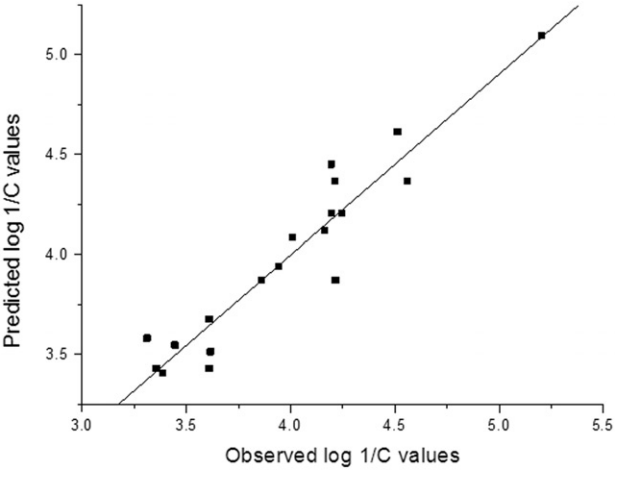

Figure 1. Plot of observed *vs.* predicted $\log 1/C$ values of the training set compounds obtained from Equation (1).

Table 7. Complete analysis of variance table of Equation (1).

	Degrees of freedom	*Sum of squares*	*Mean square*	*t-value*	*p level*
Total (corrected)	18	4.3195			
Regression	3	3.9081	1.3027		
Ix	1	1.7866	1.7866	−11.03	0.000
$B1_{R_1}$	1	1.4635	1.4635	8.51	0.000
σR_3	1	0.6579	0.6579	−4.90	0.000
Residual error	15	0.4114	0.0274		

The obtained correlation equation was screened by using a test set (Table 8) concerning the compounds **3**, **4**, **10**, **11**, **13**, **14**, **17**, and **27** that were not included in the developed model. The observed, calculated $\log 1/C$ values and residuals of the test set molecules obtained with 1 are given in Table 8. Figure 2 represents the graph of the obtained versus calculated $\log 1/C$ values of the test set molecules for the used model, which has an r value of 0.682.

The derived QSAR analysis revealed that the compounds possessing a methylene group between the phenyl and the carboxyamido moiety play a role for decreasing the activity. Consequently, it can be concluded that benzamide structure is significant for increasing potency in this set of compounds. In addition, Equation (1) demonstrates that substituent effects on the position R_1 is also important for the activity and holding a substituent possessing a minimum width property on this position like alkyl groups enhances the activity. Furthermore, substituting position R_3 with a group enhancing the electron-donor capability of the phenolic ring system plays a role for increasing the potency.

For the 3D-common feature pharmacophore hypothesis approach, the hypothesis 1 that consists one HpAr, two HBAls and HBD as shown in Figure 3a is generated as the common-feature functions to explain the specification of the antibacterial agents

Table 8. Compounds, parameters, MIC values ($\mu g\,ml^{-1}$), observed, and predicted $\log 1/C$ values of the test set by using Equation (1).

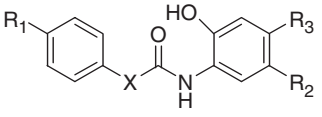

Comp. Nos	R_1	R_2	R_3	X	*MIC* $\mu g\,ml^{-1}$	Ix	σR_3	$B1_{R1}$	*Observed log 1/C*	*Calculated log 1/C*	*Residuals*
3	F	H	NO_2	–	15.6	0	0.78	1.35	4.248	3.914	0.334
4	C_2H_5	H	NO_2	–	125	0	0.78	1.52	3.360	4.075	−0.715
10	CH_3	H	NO_2	CH_2	500	1	0.78	1.52	2.757	3.135	−0.378
11	F	H	NO_2	CH_2	62.5	1	0.78	1.35	3.667	2.974	0.693
13	F	NO_2	H	CH_2	31.25	1	0	1.35	3.975	3.263	0.712
14	$C(CH_3)_3$	H	NH_2	–	7.8	0	−0.66	2.59	4.561	5.625	−1.064
17	Br	H	NH_2	–	7.8	0	−0.66	1.95	4.595	5.017	−0.422
27	F	NH_2	H	CH_2	31.25	1	0	1.35	3.920	3.263	0.657

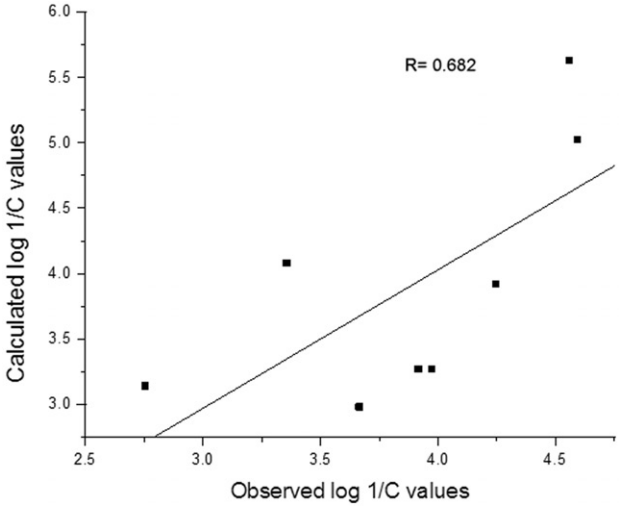

Figure 2. Plot of observed *vs.* calculated $\log 1/C$ values of the test set compounds obtained by using Equation (1).

against drug-resistant *S. aureus*. Figure 3b depicts that the most active molecule compound **1** shows a better fit with all the generated features than the rest of the compounds.

When the training compounds are mapped onto the common-feature functions generated by hypothesis 1, the HBAI feature slightly maps onto "O" of carbonyl of compounds **3**, **5**, **6**, **7**, and **15**, showing a better match for derivative 16. If the compounds possess a methylene bridge between the phenyl ring and carboxyamido moiety, then, they could not be able to show any match with this feature function. This observation explains why benzamide structure is more favourable than phenylacetamide

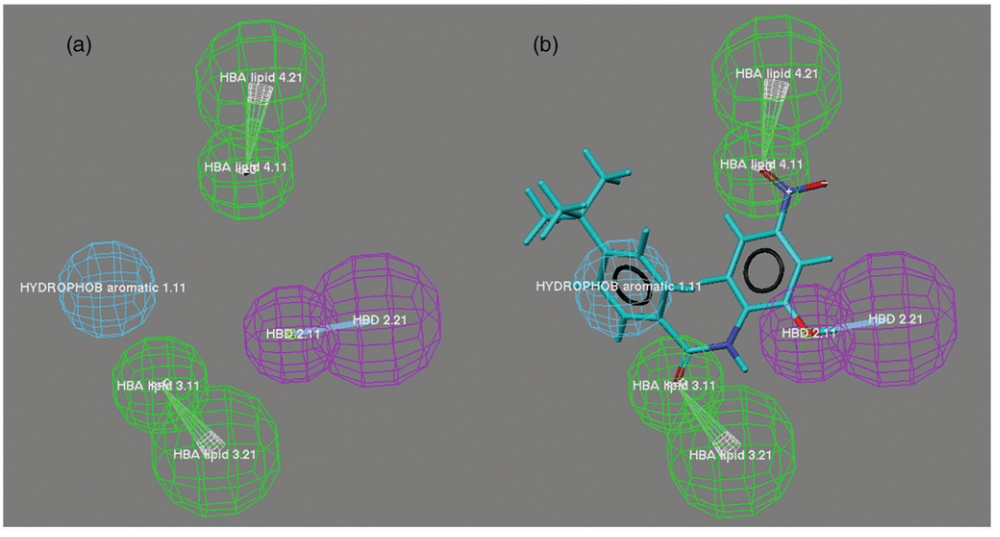

Figure 3. (a) Mapping of hypothesis 1, which contains one HpArs (blue), two HBAIs (green) and HBD (violet) pharmacophore features; (b) Mapping of compound **1** on the generated hypothesis.

for increasing potency in this set of compounds. On the other side, while NO_2 group of compounds **5**, **6**, and **7** possesses a good fit onto the other HBAI feature, the NO_2 group of structure 3 is not showing a match on this feature. Moreover, "O" of OH group on the phenyl ring of the compounds **17**, **20**, and **21** also have a pretty close fit onto this feature function. For the HBD feature, OH group of derivatives 3 and 6 map into well while the compounds **5**, **6**, **7**, and **15** show a slightly match on this feature function. Furthermore, NH_2 group of compounds **14**, **17**, and **18** is placed near to HBD feature area, however, NH_2 group of the derivatives 15 and 16 does not match with any features.

On the other side, when the less active and/or not active compounds given in Table 1 are mapped onto the generated hypothesis 1, it has been observed that they only showed a maximum match on three common features. While the NO_2 group of compounds **8**, **10**, and **12** possesses a fit onto the HBAI feature, the NO_2 group of structures 2, 4, and 9 does not show a match on this feature. As expected, the "O" of carbonyl of compounds **2** and **4** does not show a match on the other HBAI feature, because of lack of methylene bridge on their structure. All less active molecules except derivatives 8 and 10 fit with the HpAr feature as well as the OH group of compounds **2**, **4**, **8**–**10**, and **12** maps well onto the HBD feature.

In conclusion, QSAR analysis and 3D-common feature pharmacophore hypothesis generation revealed that the conformational properties of the compounds are important for the activity against drug-resistant *S. aureus* and compounds possessing a benzamide moiety rather than phenylacetamide structure increase the activity. It can be considered that holding NO_2 and OH groups on the phenyl ring that attached to the benzamide moiety is important for improving the potency against drug-resistant *S. aureus*. These observations could be useful for lead optimisation of the new candidate antibacterial agents.

References

[1] A. Dalhoff, *Quinolone resistance in Pseudomonas aeruginosa and Staphylococcus aureus, Development during therapy and clinical significance*, Infection 22 (1994), pp. 111–121.

[2] V. Lee and S. Hecker, *Antibiotic resistance versus small molecules, the chemical evolution*, J. Med. Chem. 19 (1999), pp. 521–542.

[3] D. Livermore, *Antibiotic resistance in staphylococci*, Int. J. Antimicrob. Agents 16 (2000), pp. S3–S10.

[4] K. Poole, *Multidrug resistance in gram-negative bacteria*, Curr. Opin. Microbiol. 4 (2001), pp. 500–508.

[5] D. Abbanat, M. Macielag, and K. Bush, *Novel antibacterial agents for the treatment of serious Gram-positive infections*, Expert Opin. Investig. Drugs 12 (2003), pp. 379–399.

[6] H. Mrozik et al., *A new agent for the treatment of liver fluke infection (fascioliasis)*, Experientia 25 (1969), p. 883.

[7] Japan Patent, 73, 37, 819, Chem. Abst. 81 (1974) 73387 (1973).

[8] Braz Pedido PI N80 04, 641, Chem. Abst. 95 (1981) 61812z (1981).

[9] G.A. White, *Substituted 2-methylbenzanilides and structurally related carboxamides: Inhibition of complex II activity in mitochondria from a wild-type strain and a carboxin-resistant mutant strain of Ustilago maydis*, Pest. Biochem. Physiol. 34 (1989), pp. 255–276.

[10] I. Yalcin et al., *Synthesis and microbiological activity of some novel N-(2-Hydroxyl-5-substitutedphenyl)benzacetamides, phenoxyacetamides and thiophenoxyacetamides as the possible metabolites of antimicrobial active benzoxazoles*, Il Farmaco 52 (1997), pp. 685–689.

[11] K.J. Pradhan, P.S. Variyar, and J.R. Bandekar, *Antimicrobial activity of novel phenolic compounds from green pepper (Piper nigrum L.)*, Lebensm.-Wiss. U.-Technol. 32 (1999), pp. 121–123.

[12] E. Aki Sener et al., *Synthesis and microbiological activity of some N-(o-hydroxyphenyl)benzamides and phenylacetamides as the possible metabolites of antimicrobial active benzoxazoles, Part II*, Il Farmaco 55 (2000), pp. 469–476.

[13] E. Aki-Sener et al., *Synthesis and microbiological activity of some N-(2-hydroxy-4-substitutedphenyl)benzamides, phenylacetamides and furamides as the possible metabolites of antimicrobial active benzoxazoles*, Il Farmaco 57 (2002), pp. 451–456.

[14] I. Yildiz-Oren et al., *Synthesis and microbiological activity of some substituted N-(2-hydroxy-4-nitrophenyl)benzamides and phenylacetamides as possible metabolites of antimicrobial active benzoxazoles*, Turk J. Chem. 28 (2004), pp. 441–449.

[15] I. Kobayashi et al., *In vitro anti-Helicobacter pylori activity of BAS-118, a new benzamide derivative*, J. Antimicrob. Chemoth. 50 (2002), pp. 129–132.

[16] C. Hansch and A. Leo, *Exploring QSAR: Fundamentals and applications in chemistry and biochemistry*, American Chemical Society, Washington, DC, 1995.

[17] C. Hansch and T. Fujita, *p–σ-π Analysis. A method for the correlation of biological activity and chemical structure*, J. Am. Chem. Soc. 86 (1964), pp. 1616–1626.

[18] V.E. Golender and E.R. Vorpagel, *3D-QSAR in Drug design: Theory, methods, and applications*, H. Kubinyi, ed., ESCOM Science Publishers, The Netherlands, 1993, p. 137.

[19] B. Tekiner-Gulbas et al., *QSAR of genotoxic active benzazoles*, SAR QSAR Environ. Res. 18 (2007), pp. 251–263.

[20] E.M. Krovat, K.H. Fruhwirth, and T. Langer, *Pharmacophore Identification, in silico screening, and virtual library design for inhibitors of the human factor Xa*, J. Chem. Inf. Model. 45 (2005), pp. 146–159.

[21] T. Ertan et al., *Synthesis and biological evaluation of new N-(2-hydroxy-4(or 5)-nitro/aminophenyl)benzamides and phenylacetamides as antimicrobial agents*, Bioorg. & Med. Chem. 15 (2007), pp. 2032–2044.

[22] Accelrys Inc. Catalyst 4.9 (2004).

[23] C. Hansch, A. Leo, and D. Hoekman, *Exploring QSAR: Hydrophobic, Electronic, and Steric Constants*, American Chemical Society, Washington, DC, 1995.
[24] Accelrys Inc. Cerius2 (2004).
[25] The Regression Analysis Program BILIN, http://www.kubinyi.de/bilin-program.html
[26] MINITAB Release 13.1, http://www.minitab.com
[27] N. Draper and H. Smith, *Applied Regression Analysis*, John Wiley & Sons, New York, 1966.
[28] J.O. Rawlings, *Applied Regression Analysis*, Wadsworth & Brooks/Cole, Pacific Grove, CA, 1988, pp. 186–189.
[29] S. Wold, *Validation of QSAR's*, Quant. Struct.-Act. Relat. 10 (1991), pp. 191–193.
[30] A. Smellie, S.D. Kahn, and S.L. Teig, *Analysis of conformational coverage. 1. Validation and estimation of coverage*, J. Chem. Inf. Comput. Sci. 35 (1995), pp. 285–294.
[31] A. Smellie, S.D. Kahn, and S.L. Teig, *Analysis of conformational coverage. 2. Applications of conformational models*, J. Chem. Inf. Comput. Sci. 35 (1995), pp. 295–304.
[32] A. Smellie, S.L. Teig, and P. Towbin, *Poling: Promoting conformational variation*, J. Comp. Chem. 16 (1994), pp. 171–187.
[33] J. Greene et al., *Chemical function queries for 3D database search*, J. Chem. Inf. Comput. Sci. 34 (1994), pp. 1297–1308.
[34] D. Barnum et al., *Identification of common functional configurations among molecules*, J. Chem. Inf. Comput. Sci. 36 (1996), pp. 563–571.
[35] H. Kubinyi, *QSAR: Hansch Analysis and Related Approaches*, R. Mannhold, P. Krogsgaard-Larsen, and H. Timmerman, eds., Wiley-VCH, Weinheim, 1993, pp. 91–95.
[36] H. Kubinyi, *QSAR: Hansch Analysis and Related Approaches*, R. Mannhold, P. Krogsgaard-Larsen, and H. Timmerman, eds., Wiley-VCH, Weinheim, 1993, p. 59.
[37] H. Kubinyi, *QSAR: Hansch Analysis and Related Approaches*, R. Mannhold, P. Krogsgaard-Larsen, and H. Timmerman, eds., Wiley-VCH, Weinheim, 1993, p. 63.